Polymer 50 (2009) 68–76

Contents lists available at ScienceDirect

Polymer

journal homepage: www.elsevier.com/locate/polymer

Evolution of the morphology of HIPS particles

G. Patricia Leal, José M. Asua*

Institute for Polymer Materials (POLYMAT) and Grupo de Ingeniería Química, Departamento de Química Aplicada, Facultad de Ciencias Químicas, University of the Basque Country, Apdo. 1072, ES-20080 Donostia-San Sebastián, Spain

ARTICLE INFO

Article history:
Received 4 June 2008
Received in revised form
16 October 2008
Accepted 25 October 2008
Available online 30 October 2008

Keywords:
High impact polystyrene
Phase inversion
Salami morphology

ABSTRACT

The formation and evolution of the particle morphology during the production of high impact polystyrene in bulk were investigated. Evidence about the morphology of the system during phase inversion and the subsequent evolution of the particle morphology was obtained by transmission electron microscopy in reactions in which the type and concentration of initiator, agitation speed and polybutadiene content were varied.

1. Introduction

High impact polystyrene (HIPS) is a multiphase material whose properties are largely determined by its morphology. HIPS is produced by polymerizing styrene in which some amount of polybutadiene (PBD) has been dissolved. Initially, the system is homogeneous, but as the concentration of polystyrene (PS) increases, phase separation occurs leading to a system in which the continuous phase is a solution of PBD in styrene and the dispersed phase is a solution of PS in styrene. The stability of the dispersion is greatly improved by the formation of poly(butadiene-graft-styrene) copolymers, which is promoted by using initiators able to create radicals on the PBD backbone. As polymerization proceeds, the amount of PS in the system increases and that of styrene decreases. Therefore, the volume fraction of the PS-rich phase increases and that of the PBD-rich phase decreases. At one point, a phase inversion occurs and the PS-rich phase becomes the continuous phase. The dispersed rubber particles present a complex morphology with PS occlusions. This morphology is often referred to as salami morphology. After phase inversion, polymerization proceeds until final conversion, trying to preserve the salami morphology.

Excellent reviews of the process have been published [1–4]. Kinetic models for the polymerization rate, MWD and grafting [5–7], which can be used for simulating the dynamics of continuous reactors [8–11], are available. The effect of the morphology on the properties of the HIPS has been extensively studied [12–15]. However, in spite of importance of the HIPS morphology, the effect of the process conditions on the morphology has not been extensively studied. It has been reported that particle size decreased with agitation rate [16–19]. Conflicting results on the effect of the PBD content on particle size have been reported [16,19]. Increasing initiator concentration yielded larger particle sizes [16,20]. Reiss and Graillard [16] and Moore [21] reported that the size of the rubber particles increased with the molecular weight of the PBD. Moore [21] found that salami morphologies were obtained with a first stage polymerization temperature of 60 °C, whereas very small particles with no salami morphology were obtained at 100 °C. These small particles do not provide impact strength to the HIPS. However, the effect of temperature could be counteracted by increasing the PBD concentration.

The results discussed above are difficult to interpret in mechanistic terms as the evolution of the morphology has not been studied in detail. The final morphology of the HIPS is the result of both the phase inversion and the evolution of the morphology during the second stage of the polymerization. However, no experimental evidence about the way in which phase inversion occurs has been reported. In addition, the evolution of the particle morphology after phase inversion has been scarcely studied and the studies were mostly restricted to the size of the polymer particles [18,22–24]. Lee et al. [22] used laser light scattering to monitor the time evolution of the rubber particle size distribution finding that the observed PSD became narrower and the average particles size decreased during polymerization until a stable particle size distribution was reached. The authors claimed that this evolution was linked to the phase inversion process that, because of

* Corresponding author. Tel.: +34 9 43 018 181; fax: +34 9 43 017 065.
E-mail address: jm.asua@ehu.es (J.M. Asua).

0032-3861/$ – see front matter © 2008 Elsevier Ltd. All rights reserved.
doi:10.1016/j.polymer.2008.10.035

the high viscosity of the system, spanned over a long period of time. However, the technique does not allow getting information about the internal morphology of the particles. By comparing the morphology of films formed by casting HIPS solutions with the unchanged in situ morphology, Fischer and Hellmann [23] concluded that the occlusions within the particles were stabilized by graft copolymers with one PS branch, whereas the graft copolymers with two or more PS branches were at the external interface of the polymer particles. The evolution of the particle morphology was not studied. Soto et al. [24] reported that the final particle size could be reduced by increasing agitation rate, increasing grafting efficiency (which strongly depends on the initiator used [5]) and reducing the viscosity of the system. These authors also presented TEM micrographs that showed the morphology of the particles just after the prepolymerization and at the end of the process, but its evolution was not studied.

This article is an attempt to shed light on the mechanisms ruling the formation and evolution of the particle morphology during the production of HIPS in bulk. To achieve this goal, evidence about the morphology of the system during phase inversion and the evolution of the particle morphology during the second stage polymerization was obtained by transmission electron microscopy in reactions in which the type and concentration of initiator, agitation speed and PBD content were varied.

2. Experimental

Technical grade styrene (Quimidroga), low *cis*-polybutadiene (PBD, Enichem, Intene 50A), antioxidant (Polygard, Uniroyal) and initiators (benzoyl peroxide, BPO, 97% purity, Fluka and Luperox L-256, 2,5-dimethyl-2,5-bis(2ethylhexanolperoxy)hexane, 90% purity, Arkema,) were used as-received.

Table 1 summarizes the polymerizations carried out. The polymerizations were carried out in two stages. The first one was performed in a 2 L temperature controlled stainless steel reactor. The stirrer included an anchor at the bottom and four pitched 3-blade paddles placed above the anchor. Styrene, the antioxidant and the PBD were charged to the reactor. Oxygen was removed by purging the reactor with nitrogen for 1 h. Then, the system was heated to 70 °C and kept for 3 h at 25 rpm to dissolve the PBD. The initiator dissolved in styrene was fed as a shot, the agitation rate was adjusted to the desired value (150 rpm or 250 rpm) and the temperature was raised to 90 °C at 2 °C/min. This temperature (90 ± 1 °C) was maintained for the rest of this stage, which, because of the viscosity increase, was ended at a conversion of 30–40%. The second stage of the polymerization was carried out in sealed glass vials. The reaction mixture was transferred from the reactor to the vials by using vacuum. Several vials were filled for each reaction. The vials were immersed in a thermostatic bath at 150 °C, and removed at different times to obtain samples of different conversions.

The samples withdrawn from the reactor and from the vials used for the second stage were cast on aluminium plates and the monomer was evaporated at room temperature under vacuum. The resulting films were cut into pieces and embedded in an epoxy resin that was cured overnight at 60 °C. A truncated pyramid was cut with a glass knife and stained with OsO_4 for 14 days. Then, ultrathin sections (50–170 nm thick) were cut with a diamond knife using a Leica ultracut, microtome. The samples were picked up onto 300 mesh copper grids and observed in a Hitachi 7000 FA transmission electron microscope (TEM) using an accelerating voltage of 75 kV. The average particle size and the average number of occlusions per particle were calculated from the micrographs. The observed values were affected by the fact that the particles were microtomized. If $f(R)$ is the actual particle size distribution (PSD) of the particles so that $\int f(R)\mathrm{d}R = 1$, the observed distribution of randomly cut particles is

Table 1
Polymerizations carried out.

Polymerization	Initiator	Initiator concentration (mM/L)	% PBD	Agitation rate (rpm)	Grafted PS (%)
1	L-256	1.24	6	150	15.4
2	L-256	1.24	6	250	13.4
3	L-256	2.48	6	150	16.8
4	L-256	2.48	6	250	16.8
5	BPO	1.24	6	150	15.2
6	BPO	1.24	6	250	13.2
7	BPO	2.48	6	150	17.7
8	BPO	2.48	6	250	18.4
9	L-256	1.24	9	250	23.2

$$f^*(R^*) = \frac{\int_{R^*}^{R_{max}} f(R)\mathrm{d}R}{\int_{R_{min}}^{R_{max}} \left[\int_{R^*}^{R_{max}} f(R)\mathrm{d}R\right]\mathrm{d}R^*} \quad (1)$$

where R_{max} is the radius of the largest particle and R_{min} the minimum size of the observed particles (theoretically close to zero, but in practice it is not possible to cut a tiny piece of a particle). Eq. (1) shows that the observed PSD is shifted to sizes smaller than those of the actual PSD. Therefore, the size of the particles observed in the micrographs is smaller than the actual ones. For the same reason, the apparent particle size distribution was broader than the real one. Nevertheless, comparison between observed PSDs is meaningful as the larger the particles of the latex the larger the observed ones. Similarly, the observed number of occlusions per particle was smaller than the actual one, but comparison between observed samples is also meaningful as the higher the number of occlusions in the actual particle the higher the number in the observed particles.

The percentage of solids (Eq. (2)) and the conversion of monomer (Eq. (3)) were determined gravimetrically.

$$\%\ \text{solids} = \frac{\text{total polymer}}{\text{PBD} + \text{initial styrene}} 100 \quad (2)$$

$$\%\ \text{conversion} = \frac{\text{total polymer} - \text{PBD}}{\text{initial styrene}} 100 \quad (3)$$

In order to determine the amount of PS grafted onto PBD, 0.3 g of the final HIPS were mixed under agitation for 25 h at 25 °C with 10 mL of a 50/50 vol/vol mixture of methyl-ethyl ketone and *N*,*N*-dimethylformamide containing 0.5 wt% of hydroquinone. PS is soluble in this solvent mixture whereas PBD containing chains are not soluble. The whole mixture was centrifugated at 10 000 rpm during 1 h at 10 °C. The clear solution containing the dissolved PS was separated and the PS was precipitated with methanol. The process was repeated with the fraction precipitated in the centrifugation, until no polymer precipitated when methanol was added to the clear solution. The remaining insoluble part was dried and the percentage of grafted PS was calculated as

$$\%\ \text{PS}_{\text{grafted}} = \frac{\text{weight of insoluble material} - \text{weight of PBD}}{\text{total weight of PS}} 100 \quad (4)$$

3. Results and discussion

3.1. Phase inversion

Macroscopically, phase inversion is detectable because the viscosity of the reaction mixture decreases suddenly as the polystyrene rich phase, which has a lower viscosity than the PBD-rich

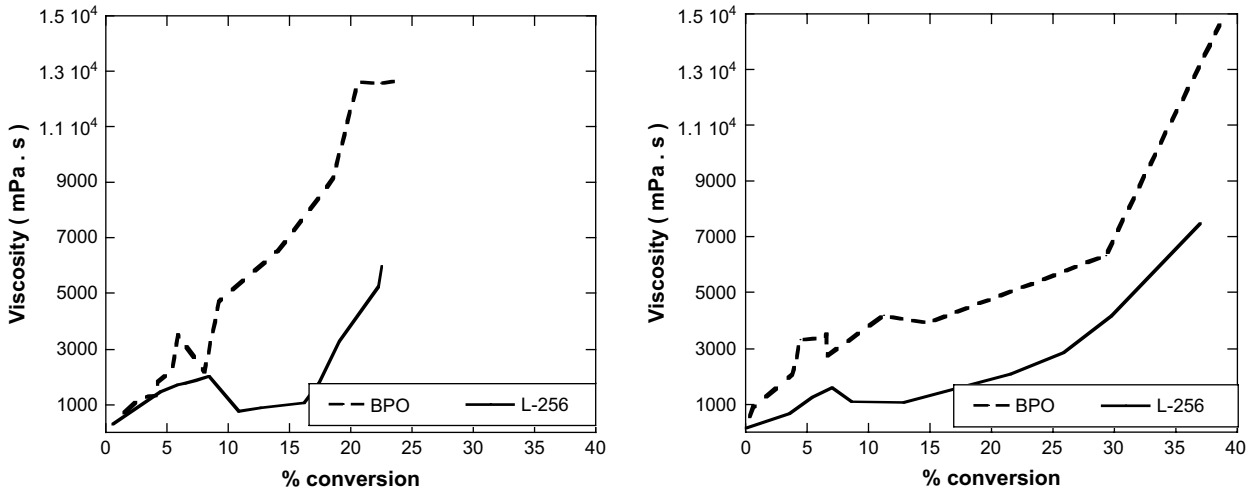

Fig. 1. Effect of the initiator type and concentration on the evolution of the viscosity (left: 1.24×10^{-3} M; right: 2.48×10^{-3} M). Lines link discrete points resulting from measurements of samples taken from the reactor.

phase, becomes the continuous phase. Under the conditions used in this work, this occurred between 5 and 10% conversion (Fig. 1). In this work, considerable effort was devoted to obtain evidence of the morphology of the system during the phase inversion only in a few cases the transition was observed (Figs. 2 and 3).

Fig. 2 presents the TEM micrographs obtained for reaction 6 at the onset of the phase inversion when the first big PS-rich aggregates were forming, but still most of the system was composed by PS particles dispersed in a PBD matrix. These dispersed particles were formed by phase separation of PS in the initial stages of the polymerization. Fig. 3 presents a more advanced moment in the phase inversion during reaction 3 in which the system is formed by a co-contiguous morphology of a PS-rich phase and a PBD-rich phase containing PS occlusions. Comparison of Figs. 2 and 3 strongly suggests that the PS occlusions within the PBD phase were the PS particles formed by phase separation during the first stages of the process.

3.2. Evolution of the particle morphology after phase inversion

3.2.1. Effect of the initiator concentration

Fig. 4 shows the evolution of the particle morphology after phase inversion in reactions 2 and 4 carried out with different initiator (L-256) concentrations (Run 2: 1.24×10^{-3} M; Run 4: 2.48×10^{-3} M) and keeping constant the rest of the variables (PBD: 6%; 250 rpm; $T = 90$ °C). Each particle was formed by a PBD matrix (dark areas in the particles) in which polystyrene occlusions (light areas within the particles) were dispersed. The continuous medium was polystyrene. It is worth pointing out that the morphologies shown in the micrographs were taken after the evaporation of the monomer, namely, the micrographs correspond to the unswollen polymer. It can be seen that after phase inversion the particles present a salami morphology that was mostly preserved during the whole process.

In order to have a more quantitative picture, the average size of the particles and the number of occlusions per particle were

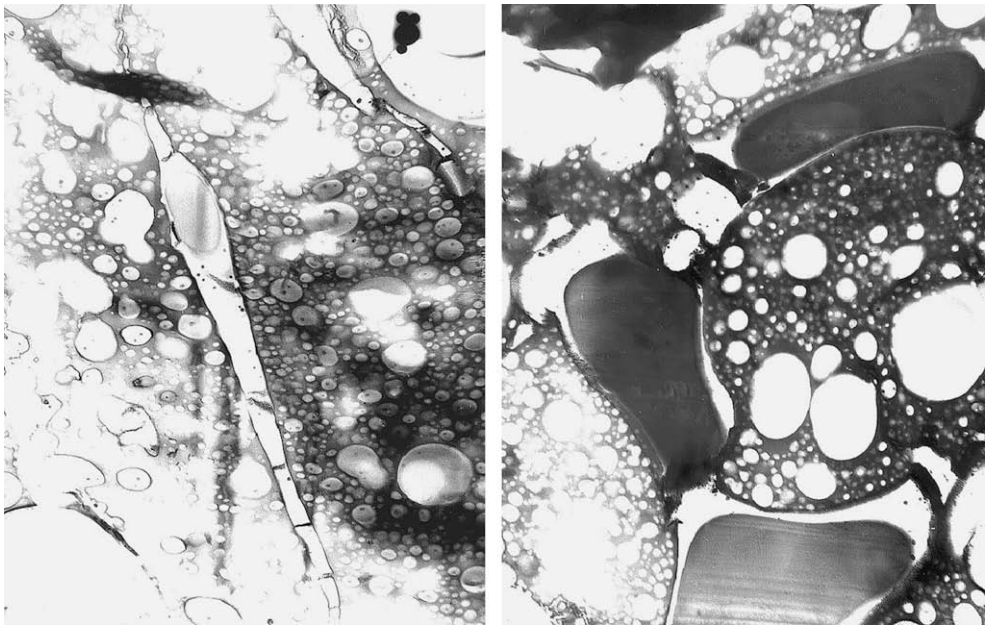

Fig. 2. TEM microphotographs for the onset of phase inversion in reaction 6 (15% solids).

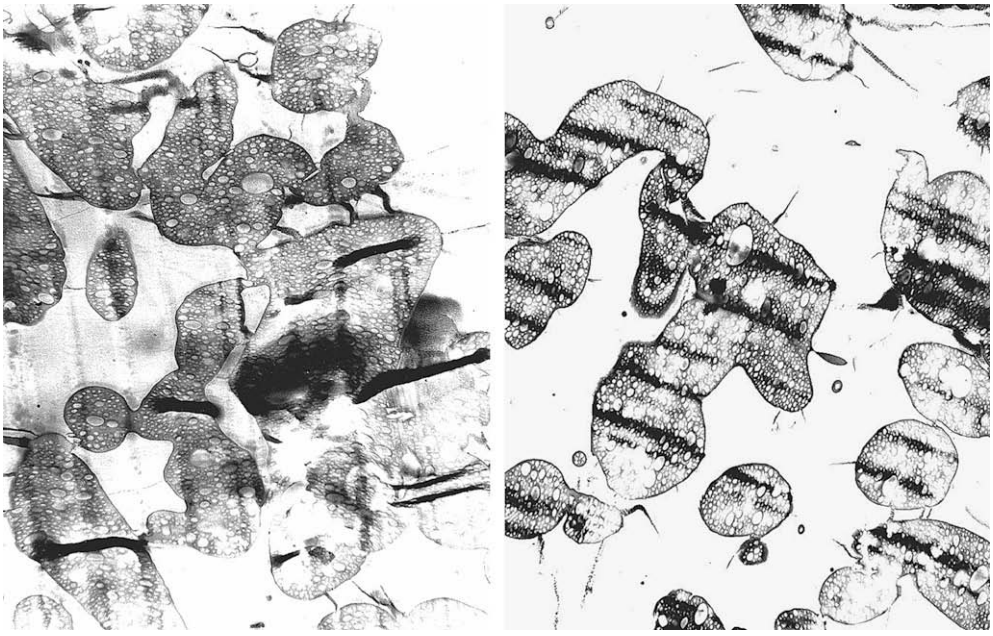

Fig. 3. TEM micrographs at advanced stages of the phase inversion in reaction 3 (18.8% solids).

determined from the micrographs counting a minimum of 400 particles using Bolero™ software. Figs. 5–7 present these results. Fig. 5 shows that the final particle size of the polymer particles increased with the concentration of initiator. This is in agreement with previous reports [16,20]. The larger size was the result of two factors. First, after phase inversion the size of the particles was larger for the higher concentration of initiator. In addition, the size of the particles remained rather constant for the lower initiator concentration whereas increased for the higher one. The size of the PS occlusions (Fig. 6) increased for both experiments being somehow larger for the reaction with higher initiator concentration. On the other hand, the number of occlusions per particle decreased during polymerization for both reactions (Fig. 7).

These results suggest the following mechanism. Polymerization starts in a solution of PBD in styrene. At one point, the polystyrene formed is not soluble in the PBD solution and phase separates forming PS-rich droplets, which are dispersed in the PBD-rich phase. The number and size of these droplets increased and at one point they start coagulating forming larger domains (Fig. 2), which eventually form a co-continuous phase with the PBD-rich phase (Fig. 3). The PBD-rich phase contains PS-rich droplets that have not coagulated to form the continuous PS phase. After completion of phase inversion, the PBD-rich phase becomes the dispersed phase, which presents a salami structure as the non-coagulated PS droplets are trapped within the PBD. In the second part of the process, the number of occlusions for particle decreases and their size increases. This strongly suggests that the occlusions coagulate between them. For analogy with the evolution of particle morphology in emulsion polymerization [25–27], the driving force can be attributed to van der Waals forces, which are attractive among occlusions. On the other hand, it is possible that some occlusions leave the particles to become part of the continuous phase as the van der Waals forces between the continuous PS phase and the PS occlusions are attractive. Actually, in some micrographs half-exited occlusions can be observed, although this may be an artefact of the sample preparation.

The van der Waals forces are proportional to the interfacial tensions between the PS and the PBD-rich phases. This interfacial tension is expected to decrease with the presence of PBD-graft-PS chains. Grafting occurs mainly by abstraction of allylic hydrogens by radicals. At the beginning of the process both initiator radicals and styryl radicals are present. At 90 °C the rate coefficient for polymer chain transfer of styryl radicals is 1400 times smaller than that of the initiator radicals (k_{tr}^{pol} = 356 L/mol s for initiator radicals and k_{tr}^{pol} = 0.25 L/mol s for styryl radicals [28]). In addition, the half-life time of the initiators used was about 1 h at 90 °C ($t_{1/2}$ = 1 h at 92 °C for BPO and $t_{1/2}$ = 1 h at 91 °C for L-256), phase inversion occurred in less than 1 h and the first polymerization stage lasted 250–500 min. Therefore, up to the phase inversion and for a large part of the first stage most of the grafting was due to the initiator radicals. By the end of the first stage, the initiator was completely consumed and hence in the second stage, radicals were produced by thermal initiation of the styrene. The reactivity of these radicals for chain transfer to PB substantially increases with temperature and at 150 °C (k_{tr}^{pol} = 8 L/mol s) [28], therefore increasing of grafting during the second stage of the process has been reported [28].

The increase in particle size with initiator concentration observed just after phase inversion (Fig. 5) may be due to the higher grafting extent (Table 1). For a given PBD concentration, the size of the particles mostly depends on the volume of the PS occlusions in the particles. The higher the grafting, the more stable the PS droplets before inversion, and hence the more likely that they do not coagulate during phase inversion. This led to a higher volume of PS occlusions in the particles, i.e., to large particles. As discussed below, viscosity (which decreased with initiator concentration) may also play a (less important) role in the size of the particles.

Fig. 5 shows that the particle size increased during polymerization in the case of the higher initiator concentration whereas remained almost constant for the smaller concentration of initiator. This means that in the latter case some occlusions left the particles. The difference was likely due to higher grafting extent at higher initiator concentration. This resulted in a smaller interfacial tension between occlusions and PBD, and hence in a smaller van der Waals force.

Figs. 2–4 seem to be in conflict with the conclusions of the work of Fischer and Hellmann [23]. According to these authors, the occlusions within the particles were stabilized by graft copolymers with one PS branch, whereas the graft copolymers with two or more PS branches were at the external interface of the polymer particles, namely the graft copolymer was segregated according to the number of branches. It is worth pointing out that graft

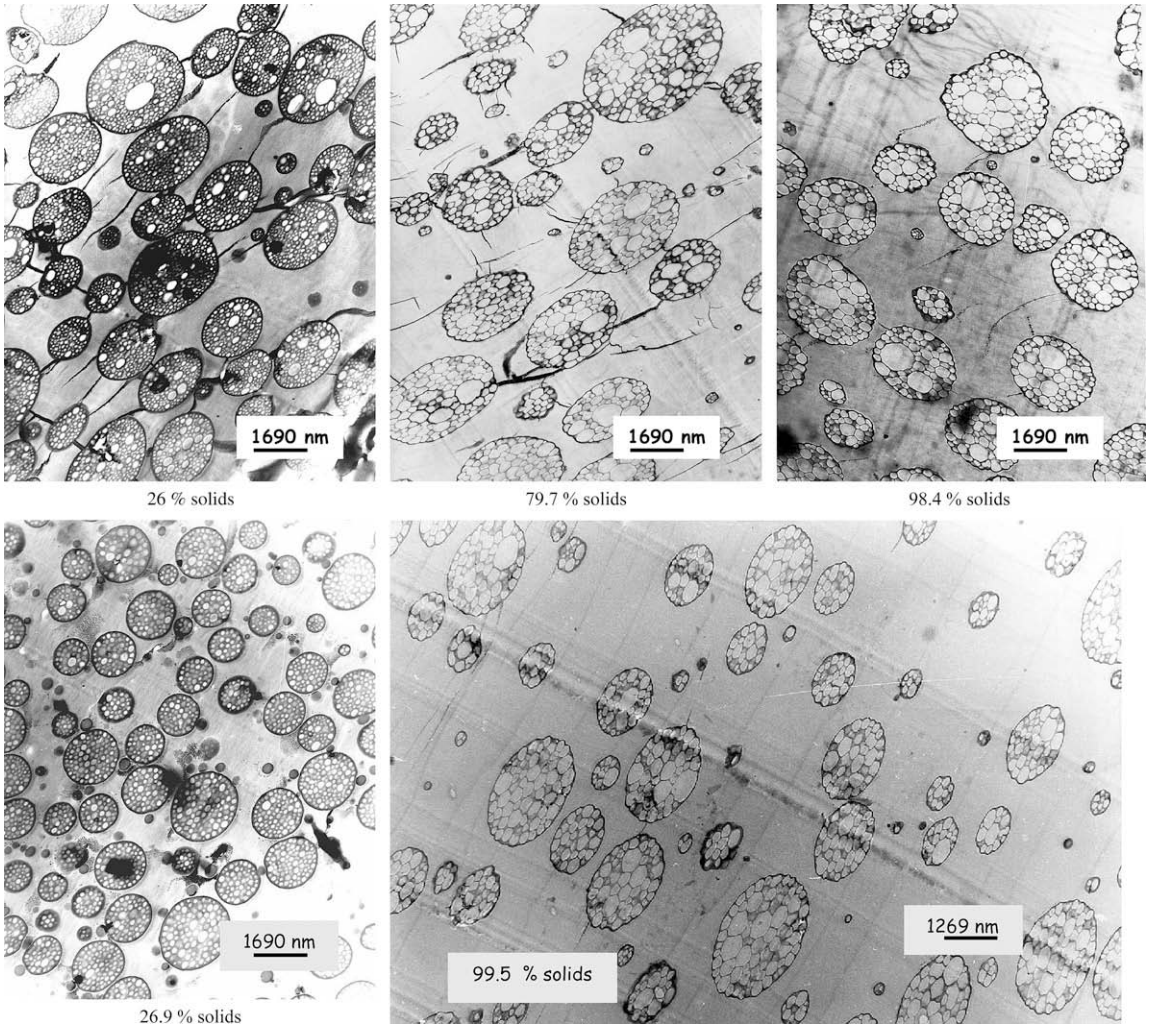

Fig. 4. Effect of the initiator (L-256) concentration on the evolution of the particle morphology (reactions 2 (1.24×10^{-3} M, lower figures) and 4 (2.48×10^{-3} M, upper figures)).

copolymers with a higher number of branches are expected to reduce more the interfacial tension between the phases and therefore to stabilize better the interface. There is no kinetic reason leading to a segregation of the graft copolymer according to the number of branches before phase inversion. Even if there would be segregation, one would expect that the PS droplets stabilized with graft copolymer containing more PS branches would be the more stable, therefore they would not contribute to the formation of the large PS domains, i.e., to the formation of the continuous PS phase.

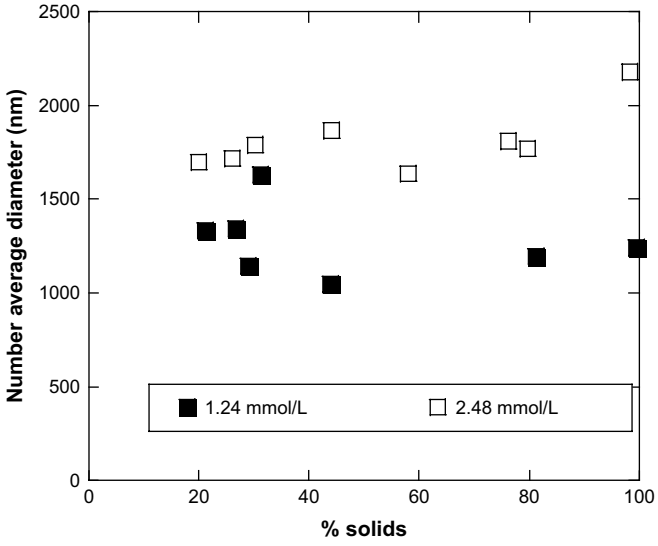

Fig. 5. Effect of the initiator concentration on the average particle size in reactions 2 (1.24×10^{-3} M) and 4 (2.48×10^{-3} M).

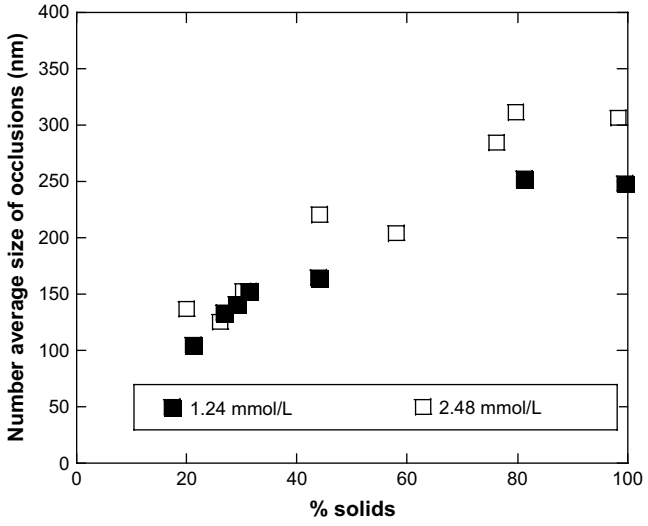

Fig. 6. Effect of the initiator concentration on the average size of the occlusions in reactions 2 (1.24×10^{-3} M) and 4 (2.48×10^{-3} M).

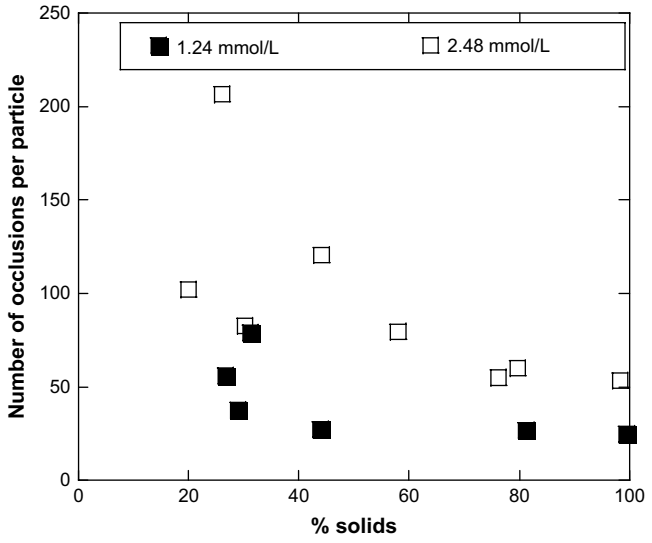

Fig. 7. Effect of the initiator concentration on the number of occlusions per particle in reactions 2 (1.24×10^{-3} M) and 4 (2.48×10^{-3} M).

The extent of grafting (i.e., the number of branches per PB chain) increases during the second stage of the process by chain transfer to polymer of the styryl radicals created by thermal initiation of styrene. Under these conditions, a preferential grafting at the external surface of the particles would require a higher concentration of styryl radicals in the continuous PS as compared with the occlusions. Considering that the interfacial area per unit volume is much higher for the occlusions, an external preferential grafting would require a much higher concentration of styryl radicals in the continuous phase. For a system in which the radicals are produced from the monomer, this means either a much higher monomer concentration or a much lower termination rate. It is worth pointing out that these are opposite requirements as higher monomer concentration would lead to lower viscosity, namely to lower gel effect. The ratio of the monomer concentrations in the continuous phase and in the occlusions can be estimated by means of the Morton equation considering the occlusions as a dispersed phase [29]. Using reasonable values for the parameters (interaction parameter = 0.35; occlusion diameter = 150 nm; interfacial tension = 5 mN/m) Morton equation predicts that the concentration of monomer in the occlusions is greater than 80% of the concentration of the monomer in the continuous phase. The concentration of radicals, [R], in the bulk polymerization of styrene at high temperature (when the radicals are created by thermal initiation of styrene) is

$$[\mathrm{R}] = \left(\frac{2k_\mathrm{I}[S]^3}{k_\mathrm{t}}\right)^{1/2}$$

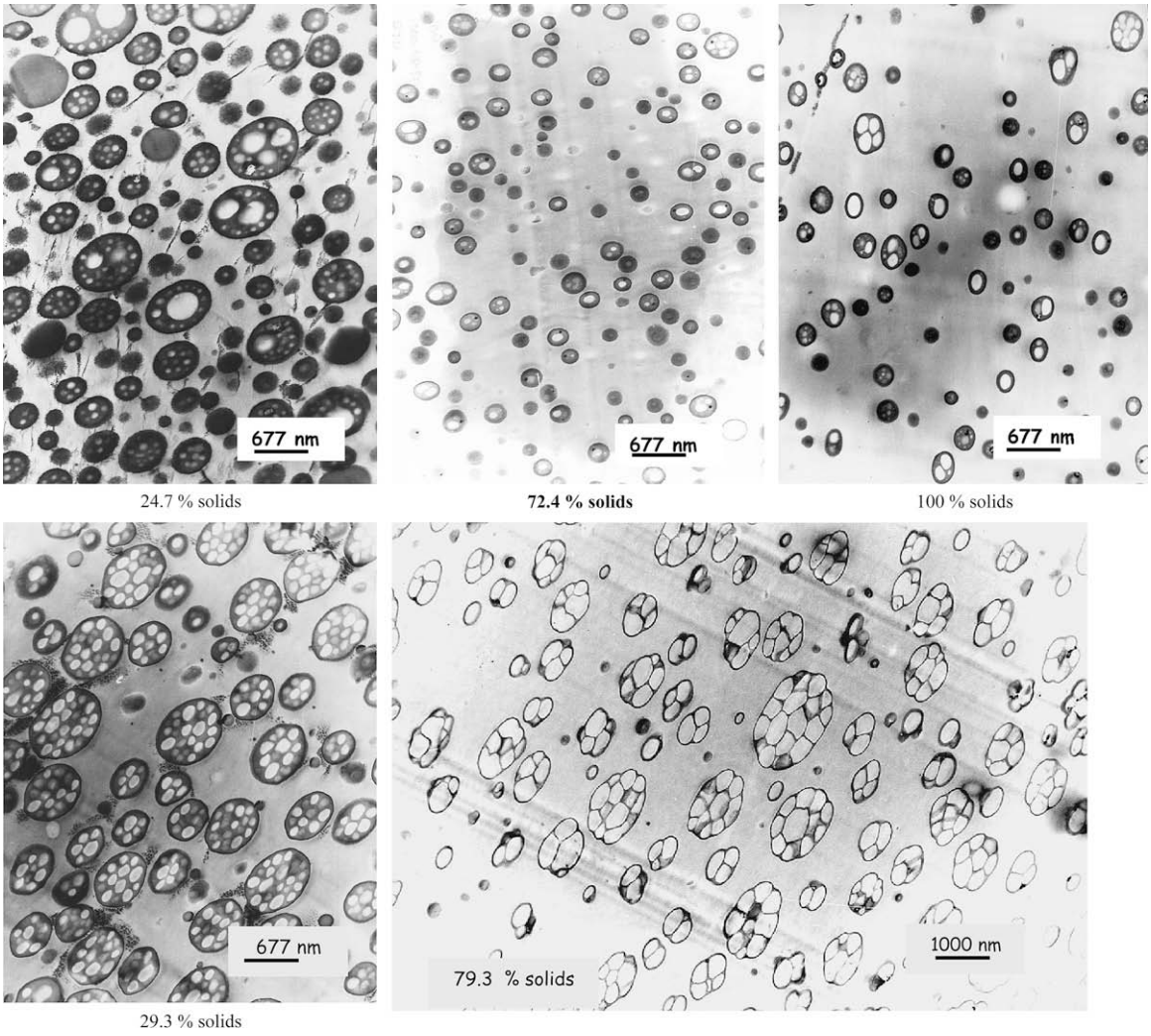

Fig. 8. Effect of the initiator (BPO) concentration on the evolution of the particle morphology (reactions 6 (1.24×10^{-3} M, upper figures) and 8 (2.48×10^{-3} M, lower figures)).

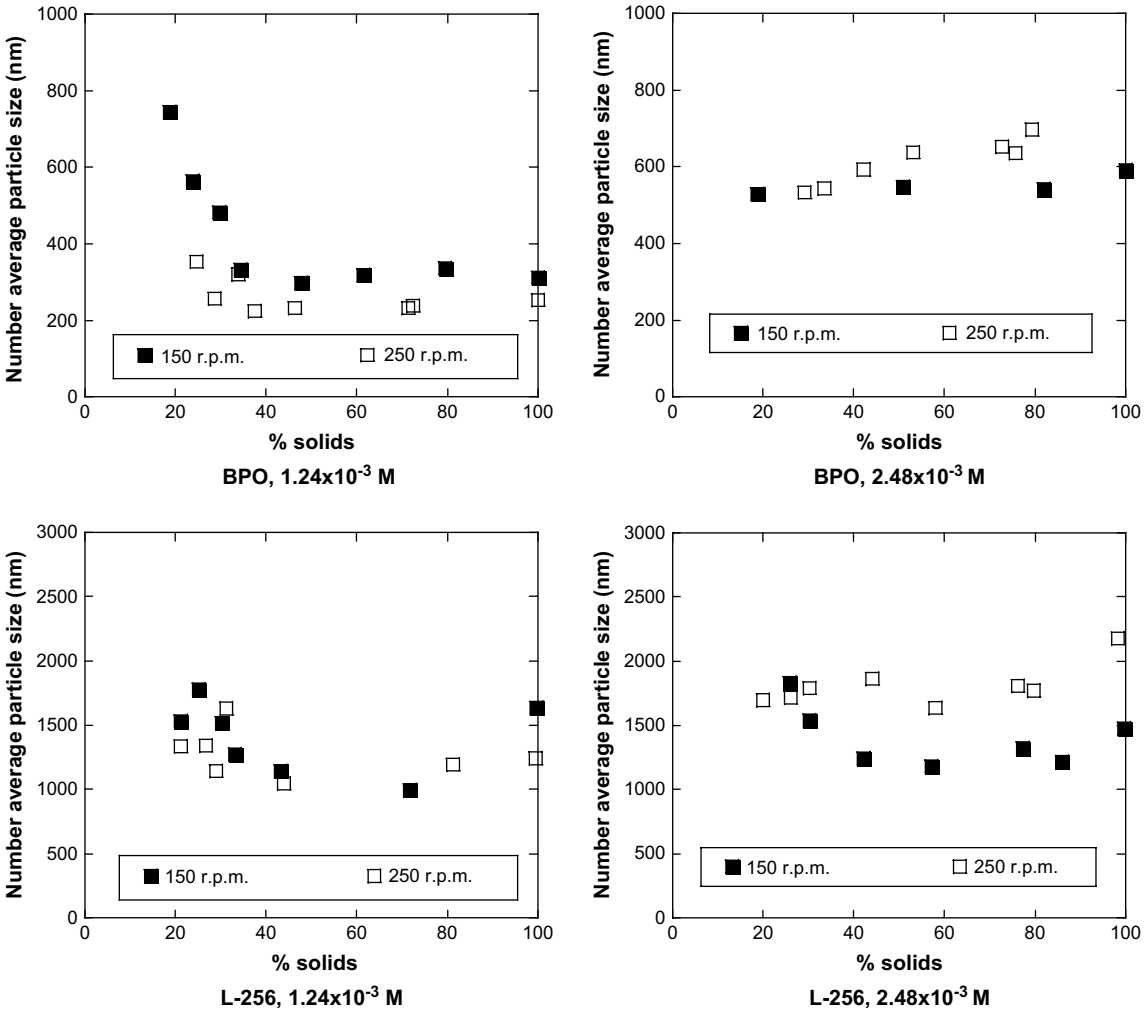

Fig. 9. Effect of the agitation rate on the particle size.

where k_i is the rate constant for thermal initiation of styrene, [S] the concentration of styrene and k_t the termination rate constant. Therefore, if the concentration of styrene in the occlusions is 80% of that in the continuous phase, the radical concentration ratio is:

$$\frac{[R]_{continuous}}{[R]_{occlusion}} = 1.39\left(\frac{k_{tocclusion}}{k_{tcontinuous}}\right)^{1/2}$$

$k_{tocclusion}$ should be lower than $k_{tcontinuous}$ because of the stronger gel effect in the occlusions (lower styrene concentration). For the sake of comparison, let us consider a concentration of styrene in the continuous phase equivalent to a conversion of 70%. In this case, $k_{tocclusion}/k_{tcontinuous}$ phase = 0.62 [30]. Therefore, $[R]_{continuous}/[R]_{occlusion} = 1.1$, which does not justify a significant variation in the number of branches.

3.2.2. Effect of the initiator type

Fig. 8 presents the evolution of the HIPS morphology in reactions 6 and 8 that used BPO as initiator. Comparison with Fig. 4 shows that just after phase inversion, the size of the particles obtained with BPO was smaller than with L-256. In the phase inversion of polymer blends, it has been reported that particle size was minimum when the viscosity ratio was close to unity [31]. The viscosity ratio between the PBD-rich phase and the PS-rich phase can be estimated from Fig. 1 by considering that the viscosity at the point of break (beginning of the phase inversion) corresponded to the PBD-rich phase and that of the minimum after phase inversion corresponded to the PS-rich phase. In all cases, the viscosity ratio was higher for L-256, which would lead to larger particles, but the differences $((\eta_{PBD}/\eta_{PS})_{L\text{-}256} = 2.5;\ (\eta_{PBD}/\eta_{PS})_{BPO} = 1.6)$ seem to be small to justify the substantial variation in particle size observed. Another factor affecting particle size and morphology is the graft copolymer. Table 1 shows that the type of initiator had no a substantial effect on the level of grafting at the end of the process. However, it has been reported that L-256 yields a higher grafting than monofunctional initiators such as BPO [20]. This means that during the first stage and mainly before the phase inversion, the graft copolymer formed with BPO was less efficient stabilizing the interface PS–PBD than that formed with L-256. This would result in less stable PS droplets, which would mostly coagulate during phase inversion to produce the continuous phase. As the size of the particles mainly depends on the volume of the PS occlusions, the resulting particles would be smaller than those obtained with L-256.

The evolution of the particle morphology in Fig. 8 supports the hypothesis that the graft copolymer formed with BPO was less efficient stabilizing the PS–PBD interface, as substantial coalescence of occlusions was observed for the higher concentration of BPO (2.48×10^{-3} M), while Fig. 4 shows that for the same concentration of L-256 a stable and well developed salami morphology was achieved. For $C_{BPO} = 1.24 \times 10^{-3}$ M, the particles lost most of their occlusions, whereas for the same concentration of L-256 a well developed salami morphology was obtained at the end of the process.

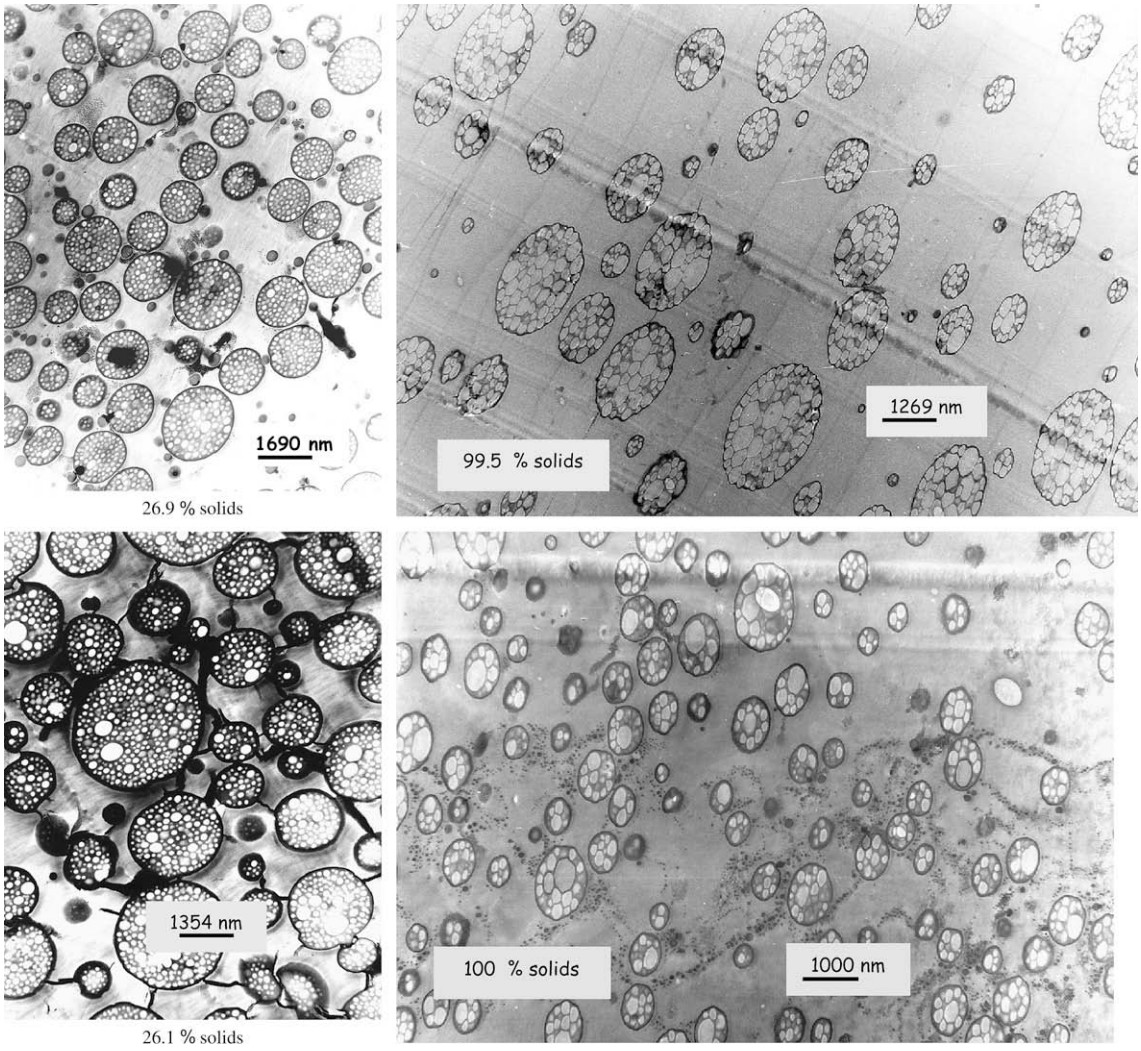

Fig. 10. Effect of the concentration of PBD on the evolution of the particle morphology (reactions 4 (6 wt%, upper figures) and 9 (9 wt%, lower figures)).

It may be argued that polymerization kinetics is also playing a role as polymerizations using L-256 were 30% faster than those using BPO, which would allow more time to the occlusions to leave the particles, in the case of BPO. However, reaction 6 (with BPO, 2.48×10^{-3} M) was faster than reaction 2 (with L-256, 1.24×10^{-3} M) and the salami morphology was relatively well preserved in reaction 2, whereas it was lost in reaction 6. Therefore, the difference observed should be a matter of the effect of initiator on grafting.

3.2.3. *Effect of the agitation rate*

Fig. 9 presents the effect of the agitation rate on the evolution of the particle diameter. It can be seen that, contrary to what has been reported in literature [16–19] for the range of agitation rates studied, the effect was negligible for the lower initiator concentration and weak for the higher concentration of initiator. An explanation of this behaviour is as follows. The particle size achieved by mechanical dispersion is the result of the interplay between droplet break-up and coalescence, the final size being determined by the mechanism giving the largest droplet size [32]. Droplet break-up is the size-controlling mechanism when the droplets formed are very stable. In this case, droplet size decreases with agitation rate. On the other hand, droplet coagulation is the size-controlling mechanism when the concentration of the stabilizing grafted copolymer is not enough to stabilize the droplets formed by intensive droplet break-up. In this case, droplet size is independent of the agitation rate. It looks that this is our case, likely due to the fact that a well-mixed laboratory reactor was used.

3.2.4. *Effect of the concentration of PBD*

Fig. 10 shows the effect of the concentration of PBD on the evolution of the particle morphology. It can be seen that well developed salami morphologies were developed after phase inversion. The subsequent evolution was critically affected by the concentration of PBD. With a 6 wt% (reaction 2) the salami morphology was relatively well preserved during the whole process, whereas at higher PBD concentration (9 wt%, reaction 9) most of the PS occlusions left the particles and at the end of the process small particles containing a few PS occlusions were obtained. Table 1 shows that the fraction of PS grafted on the PBD chains increased with the PBD concentration, although the amount of PS grafted per unit mass of PBD decreased with PBD concentration. This may result in a less efficient compatibilizer. In addition, PBD may form an elastic crosslinked network that may create an additional force to expel the occlusions to the continuous phase.

4. Conclusions

The evolution of the particle morphology during the production of HIPS was monitored by TEM. The morphologies observed suggest that polymerization starts in a solution of PBD in styrene. At one point, the polystyrene formed is not soluble in the PBD solution and

phase separates forming PS-rich droplets, which are dispersed in the PBD-rich phase. These droplets are stabilized by PBD-graft-PS copolymers formed in situ. The number and size of these droplets increased and at one point they start coagulating forming larger domains, which eventually form a co-continuous phase with the PBD-rich phase. The PBD-rich phase contains PS-rich droplets that have not coagulated to form the continuous PS phase. After completion of phase inversion, the PBD-rich phase becomes the dispersed phase, which presents a salami structure as the non-coagulated PS droplets are trapped within the PBD. In the second part of the process, the occlusions coagulate between them and some of them leave the particles to become part of the continuous phase. Van der Waals forces may be the driving force for these processes. These two processes and the morphology achieved immediately after phase inversion determine the final morphology of the HIPS. The extent of grafting is the key factor for controlling the whole morphology. The higher the grafting the higher the stability of the PS–PBD interface and the more developed salami morphologies can be obtained. Initiator type and concentration and PBD concentration were the main process variables controlling grafting, and hence particle morphology. Agitation showed almost no effect under the conditions investigated.

Acknowledgements

G.P. Leal acknowledges the AECI grant. Financial support from MEC (CTQ2006-03412) and Diputación Foral de Gipuzkoa is greatly appreciated.

References

[1] Martin MF, Viola JP, Wuensch JR. In: Scheirs J, Priddy D, editors. Modern styrenics polymers: polystyrenes and styrenic copolymers. Chisterter: J. Wiley; 2003.
[2] Maul J, Frushour BG, Kontoff H, Eichenauer KHO. Ullmann's encyclopedia of industrial chemistry. 7th ed. Weinheim: Wiley-VCH; 2004.
[3] Meira GR, Kiparissides C. In: Asua JM, editor. Polymer reaction engineering. Oxford: Blackwell Publishing; 2007.
[4] Meira GR, Luciani CV, Estenoz DA. Macromol React Eng 2007;1:25–39.
[5] Huang NJ, Sundberg Dc. J Polym Sci Part A Polym Chem 1995;33:2571–86.
[6] Estenoz DA, Gonzalez IM, Oliva HM, Meira Gr. J Appl Polym Sci 1999;74:1950–61.
[7] Casis N, Estenoz D, Gugliotta L, Oliva H, Meira Gr. J Appl Polym Sci 2006; 99:3023–39.
[8] Estenoz DA, Meira GR, Gomez N, Oliva HM. AIChE J 1998;44:427–41.
[9] Verazaluce-Garcia JC, Flores-Tlacuahuac A, Saldivar-Guerra E. Ind Eng Chem Res 2000;39:1972–9.
[10] Luciani CV, Estenoz DA, Meira GR, Oliva HM. Ind Eng Chem Res 2005;44:8354–67.
[11] Flores-Tlacuahuac A, Biegler LT, Saldivar-Guerra E. Ind Eng Chem Res 2006; 45:6175–89.
[12] Chang EP, Takahashi A. Polym Eng Sci 1978;18:350–4.
[13] Enal'ev VD, Noskova NA, Mel'nichenko VI, Zhuravel YN, Bulatova VM. Org Coat Plast Chem 1979;40:848–53.
[14] Cook DG, Plumtree A, Rudin A. Plast Rubber Comp Process Appl 1993;20: 219–27.
[15] Choi JH, Ahn KH, Kim SY. Polymer 2000;41:5229–35.
[16] Reiss G, Graillard P. In: Reichert KH, Geiseler GW, editors. Polymer reaction engineering. Basel: Hüthing &Wepf; 1983. p. 221.
[17] Silberberg J, Han Cd. J Appl Polym Sci 1978;22:599–609.
[18] Sardelis K, Michels HJ, Allen G. J Appl Polym Sci 1983;28:3255–68.
[19] Jeoung HG, Chung D, Ahn KH, Lee S. J Polym (Korea) 2001;25:744–53.
[20] Estenoz DA, Leal GP, López YR, Oliva HM, Meira Gr. J Appl Polym Sci 1996;62:917–39.
[21] Moore JD. Polymer 1971;12:478–86.
[22] Lee SJ, Chun BC, Ahn KH, Lee Sj. J Chem Eng Jpn 2004;37:217–23.
[23] Fischer M, Hellmann GP. Macromolecules 1996;29:2498–509.
[24] Soto G, Nava E, Rosas M, Fuenmayor M, Gonzalez IM, Meira GR, et al. J Appl Polym Sci 2004;92:1397–412.
[25] González-Ortiz LJ, Asua JM. Macromolecules 1995;28:3135–45.
[26] González-Ortiz LJ, Asua JM. Macromolecules 1996;29:383–9.
[27] González-Ortiz LJ, Asua JM. Macromolecules 1996;29:4520–7.
[28] Estenoz DA, Oliva HM, Meira Gr. J Appl Polym Sci 1996;59:861–85.
[29] Morton M, Kaizermann S, Altier Mw. J Colloid Interface Sci 1954;9:300–12.
[30] Friis N, Hamielec AE. In: Piirma I, Gardon JL, editors. Emulsion polymerization. ACS Symposium Series, vol. 24; 1976. p. 82–91.
[31] Zhang X, Yin Z, Yin J. J Appl Polym Sci 1996;62:893–901.
[32] Manea M, Chemtob A, Paulis M, de la Cal JC, Barandiaran MJ, Asua JM. AIChE J 2008;54:289–97.